ELSEVIER

Journal of Photochemistry and Photobiology A: Chemistry 142 (2001) 1–8

Journal of Photochemistry and Photobiology A:Chemistry

www.elsevier.com/locate/jphotochem

# Kinetic measurements of fluorine, bromine and iodine atom-abstraction reactions at elevated temperatures by ground-state atomic rubidium, Rb($5^2S_{1/2}$), studied by time-resolved laser-induced fluorescence

E. Martinez [a], J. Albaladejo [a], E. Jimenez [a], A. Notario [a], D. Husain [b,*], K.M.N. De Silva [b]

[a] *Departamento de Química Física, Universidad de Castilla-La Mancha, Campus Universitario s/n, 13071 Ciudad Real, Spain*
[b] *Department of Chemistry, University of Cambridge, Lensfield Road, Cambridge CB2 1EW, UK*

Received 24 January 2001; received in revised form 23 May 2001; accepted 30 May 2001

**Abstract**

The kinetics of a range of halogen atom-abstraction reactions undergone by atomic rubidium in its electronic ground state, Rb($5^2S_{1/2}$), have been investigated by time-resolved laser-induced fluorescence at elevated temperatures. Rb($5^2S_{1/2}$) was generated in an excess of halogenated reactant and He buffer gas by pulsed photolysis of rubidium halide vapours. Two separate experimental systems were employed operating at the Rydberg transition at $\lambda = 420.2$ nm {Rb[6p($^2P_{3/2}$)] $\rightarrow$ Rb[5s($^2S_{1/2}$)]} and at the shorter wavelength component of the spin-orbit resolved D-line doublet transition at $\lambda = 780.0$ nm {Rb[5s5p($^2P_{3/2}$)] $\rightarrow$ Rb[5s($^2S_{1/2}$)]}. Second-order rate constants $k_{RX}$ for various F, Br and I abstraction reactions have been measured for essentially single-temperature conditions. These rate constants, which represent a new body of absolute rate data for Rb($^2S_{1/2}$), are compared with the values reported hitherto by time-resolved atomic resonance absorption spectroscopy and with those previously obtained for other alkali metal atoms using time-resolved techniques. 

*Keywords:* Kinetic measurements; Laser-induced fluorescence; Ground-state atomic rubidium; Halogen atom abstraction

## 1. Introduction

Absolute rate data resulting from time-resolved investigations on alkali atoms in the gas phase have been reported for a wide range of atomic reactions for both their fundamental importance and their roles in atmospheric chemistry and flame inhibition processes [1–3]. Emphasis has understandably been given to rate processes undergone by the lighter alkali atoms. Reactions of the heavier Rb($5^2S_{1/2}$) atom, investigated by time-resolved techniques, have been less widely studied. Davidovits and co-workers have reported studies of the reactions of alkali metal atoms in general with $Cl_2$, $Br_2$ and $I_2$ using flash photolysis (FP) and atomic resonance absorption (ARA) spectroscopy [4–7]. Husain et al. [8–11] subsequently reported the kinetic studies of halogen atom-abstraction reactions by alkali metals atoms with alkyl halides and mixed halides of fluorocarbons using a modified system from that originally described by Davidovits [4–7]. Absolute rate constants for the third-order recombination reactions Rb + OH + He [12] and Rb + I + He [13] have also been reported using time-resolved molecular and atomic fluorescence for OH and I, respectively, in the presence of excess Rb and He. Recently, kinetic studies on the reactivity of Rb with a series of alkyl chlorides [14] and alkyl bromides [15], in which the length of the aliphatic chain was varied, have been performed using the FP/laser-induced fluorescence (LIF) technique. We have also recently reported a measurement of the absolute rate constant for the reaction between Rb + $N_2O$ with this technique [16] where the result has been compared with earlier measurements using time-resolved ARA spectroscopy [17].

In this paper, we report the results of kinetic studies at elevated temperatures of reactions of Rb($5^2S_{1/2}$) with halogenated reactants involving F, Br and I derivatives employing the FP/LIF technique, namely, with the species $CF_4$,

* Corresponding author. Tel.: +44-1223-336463; fax: +44-1223-336362.

1010-6030/01/$ – see front matter 
PII: S1010-6030(01)00488-9

$CF_3H$, $CF_2H_2$, $CF_3H$, $CF_3Br$, $CF_2Br_2$, $CFBr_3$, $CH_2Br_2$, $C_2H_4Br_2$, $CH_3I$ and $CH_2I_2$. Some of these processes have previously been studied by time-resolved ARA [18] but kinetic measurements involving time-resolved LIF have not been reported hitherto. The absolute rate data reported here are compared, where possible, with second-order rate constants for $Rb(5^2S_{1/2})$ reported hitherto by ARA though such data are limited. The results are also compared with those previously obtained for other alkali metals using different time-resolved spectroscopic techniques.

## 2. Experimental

Two systems were employed using FP with pulsed LIF for atomic monitoring in the time-domain. The first, system A, which was previously constructed for kinetic investigations on $Cs(6^2S_{1/2})$ [19–21], was modified for the detection of $Rb(5^2S_{1/2})$ on studies with the molecules $CF_4$, $CF_3H$, $CF_2H_2$, $CH_3F$, $CF_3Br$, $CF_2Br_2$ and $CFBr_3$. A schematic representation of the apparatus is shown in Fig. 1 and only a brief description will be given here. Rb atoms were generated by FP of a rubidium halide vapour in equilibrium with its solid at elevated temperatures (780–830 K) [22–24] using a high pressure Xe flash lamp system (Optoelektronik, model JML-SP10, pulse energy 1.25 J). All the rubidium halides are characterised by high absorption cross-sections in the ultra-violet [25]. The temperature was measured with a calibrated thermocouple and regulated (±5 K) by means of a temperature controller (Jumo, model dTRON16). Atomic rubidium was monitored using the Rydberg transition at $\lambda = 420.2$ nm ($6^2P_{3/2} \leftarrow 5^2S_{1/2}$) employing a pulsed dye-laser (Continuum ND60, 1 mJ/pulse at 5 Hz, Stylbene 420) pumped by a Nd:YAG laser (Continuum NY 81CS10). LIF signals were collected orthogonal to the photolysis and probe beams and passed through an interference filter (420.2 nm transmission peak, FWHM 2 nm) and a gated photomultiplier tube (Thorn EMI 9813B, Bialk.). The signal from the photomultiplier tube was fed into a gated integrator and then directed to a microcomputer for data analysis. The timing sequence for the pulsed irradiation, photomultiplier gating, laser probing and procedure for pulse control, together with signal capture using boxcar integration, critical to the experimental arrangement, have been previously described in detail [19–21].

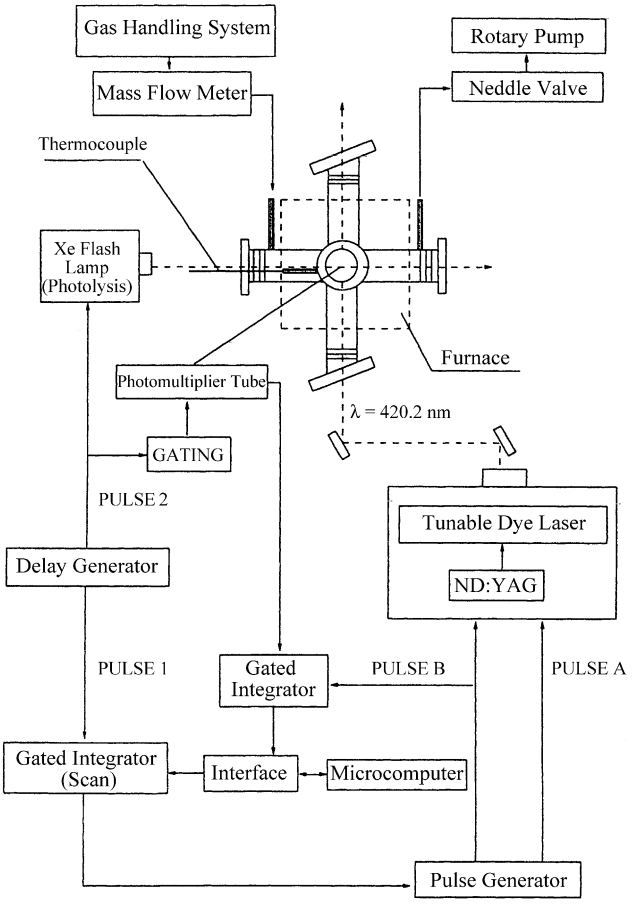


Fig. 1. Block diagram of the experimental system employed for the kinetic study of $Rb(5^2S_{1/2})$ at elevated temperatures, generated by FP of a rubidium halide and monitored by time-resolved LIF at $\lambda = 420.2$ nm $\{Rb[6p(^2P_{3/2})] \rightarrow Rb[5s(^2S_{1/2})]\}$.

The second apparatus (B) employed for the kinetic study of $Rb(5^2S_{1/2})$ with $CF_3Br$ ($T = 875$ K), $CH_2Br_2$, $C_2H_4Br_2$, $CH_3I$ and $CH_2I_2$ using the FP/LIF method has been described in earlier papers [14,15] and its operation is only summarised here. $Rb(^2S)$ was generated by the repetitive pulsed irradiation of the rubidium halide vapour at a somewhat higher energy ($E = 12$ J, 5 Hz) using an ultra-violet flash lamp, externally triggered. The atom was again monitored by the LIF technique, now at the shorter wavelength component of the D-line doublet transitions $\{Rb(5^2P_{3/2}) - Rb(5^2S_{1/2})\}$ at $\lambda = 780.0$ nm [14,15]. This was generated using a tuneable pulsed dye-laser pumped by a pulsed Nd-YAG laser operating at $\lambda = 532$ nm. LDS 765 (Exciton) laser dye was used and the dye laser was employed at energies of less than 1 mJ per pulse to avoid any saturation effects. The fluorescence signals were optically isolated by means of an interference filter prior to detection by a 'gated' photomultiplier tube (E.M.I. 9558B, S20 response). The resulting output voltage was displayed on an oscilloscope and input into the gated integrator of a boxcar averager. The signal was then transferred to a computer and the data acquisition was controlled by a commercial software package specifically written for use with the boxcar integrator system. The details of the timing procedure for the various pulses have been given [14,15] as have the construction of the atomic decay profiles. With exceptions, dependence of the absolute second-order rate constants on temperature could not normally be characterised with either systems A and B on account of the narrow temperature ranges accessible. Hence, the values of rate constants for reactions of $Rb(5^2S_{1/2}) + RX$, $k_{RX}$, reported here, for various F, Br and I abstraction reactions are essentially single-temperature determinations, yielding the following results:

| Reactant | $T$ (K) | $k_{RX}$ (cm$^3$ molecule$^{-1}$ s$^{-1}$) |
|---|---|---|
| $CF_4$ | 780 | $(4.8 \pm 1.4) \times 10^{-15}$ |
| $CF_3H$ | 780 | $(9.9 \pm 1.4) \times 10^{-14}$ |
| $CF_2H_2$ | 780 | $(9.7 \pm 3.4) \times 10^{-13}$ |
| $CH_3F$ | 780 | $(1.1 \pm 0.6) \times 10^{-12}$ |
| $CF_3Br$ | 830 | $(6.9 \pm 0.9) \times 10^{-12}$ |
| | 875 | $(1.9 \pm 0.2) \times 10^{-11}$ |
| $CF_2Br_2$ | 780 | $(2.9 \pm 1.6) \times 10^{-11}$ |
| $CFBr_3$ | 780 | $(4.3 \pm 2.8) \times 10^{-11}$ |
| $CH_2Br_2$ | 876 | $(9.9 \pm 0.2) \times 10^{-12}$ |
| $C_2H_4Br_2$ | 876 | $(8.5 \pm 0.4) \times 10^{-12}$ |
| $CH_3I$ | 875 | $(1.1 \pm 0.2) \times 10^{-11}$ |
| $CH_2I_2$ | 875 | $(9.1 \pm 0.1) \times 10^{-12}$ |

### 2.1. Materials

Helium (purity, 99.999%; Distillers M.G. and Carburos Metalicos) was used without purification. The photochemical precursors, RbBr (99.7%, Aldrich) and RbI (Aldrich, 99.9%), was refluxed in the reactor at ca. 800 K for several hours prior to kinetic measurements. $CF_4$ (99.98%), $CF_3H$ (99%), $CF_2H_2$ (98%), $CH_3F$ (99%) (Argon S.A.), $CF_3Br$ (99.7% Argon S.A. and 99.99% Matheson), $CH_2Br_2$ (99.0%), $C_2H_4Br_2$ (99.0%) $CH_3I$ (99.0%) and $CH_2I_2$ (99.0%) (Aldrich) were used as supplied following degassing by numerous freeze–pump–thaw cycles (FPT) at 77 K. Liquid samples of $CF_2Br_2$ (97%, Aldrich) and $CFBr_3$ (99%, Aldrich) were purified by trap-to-trap distillation before use.

## 3. Results

Time-resolved LIF measurements on Rb($5^2S_{1/2}$) were carried out under pseudo-first-order conditions with reactant concentrations factor of at least $10^3$ in excess over that of Rb, photochemically generated and removed as follows:

$$RbBr, RbI + h\nu(\lambda \geq 190\,nm) \rightarrow Rb(5^2S_{1/2}) + Br, I \quad (1)$$

$$Rb(5^2S_{1/2}) + RX \rightarrow RbX + R \quad (k_{RX}) \quad (2)$$

$$Rb(5^2S_{1/2}) \rightarrow \text{diffusional loss} \quad (3)$$

Time scales used were sufficiently long to ensure that relaxation of any Rb($5^2P_J$) and the higher lying spin-orbit states, Br($4^2P_{1/2}$) and I($5^2P_{1/2}$), was rapid compared to the rate of chemical removal of Rb($5^2S_{1/2}$). Under these experimental conditions, the decay of the Rb atom concentration is given by the integrated expression:

$$[Rb]_t = [Rb]_{t=0} \exp(-k't) \quad (4)$$

where $k'$ is the overall pseudo-first-order rate coefficient of the atom. This is related to the second-order rate constant for the general reaction (3), $k_{RX}$, by the standard expression

$$k' = k_{diff} + k_{RX}[RX] \quad (5)$$

where $k_{diff}$ is the first-order rate coefficient for the removal of Rb($5^2S_{1/2}$) in the absence of added reactant, primarily attributed to diffusion out of the viewing zone, which is inversely proportional to the total pressure, $p_T$ ($k_{diff} = \beta/p_T$).

Values of $k'$ were obtained from exponential fittings of the LIF signals recorded at varying total pressures within the limited temperature range 780–876 K in the presence of a fixed fractional composition of the halogenated reactant ($f = [RX]/([RX]+[He])$) as hitherto [14,15,19–21]. Thus, for a series of such measurements, Eq. (5) can be expressed in terms of $p_T$ in the form

$$k' p_T = \beta + k_{RX} {p_T}^2 \quad (6)$$

where $k_{RX}$ is now in the appropriate units involving pressure and $\beta$ is linearly related to the binary diffusion coefficient of Rb atoms in helium, $D_{12}$(Rb–He) [14,16]. Hence, $k_{RX}$ may be evaluated from the slopes of plots of $k'p_T$ vs. ${p_T}^2$ plots for a given temperature and using the appropriate value of $f$. Detailed investigation of $D_{12}$(Rb–He) using the 'long-time solution' of the diffusion equation is not pursued in the present measurements in view of the difficulty in characterising the appropriate boundary conditions concerned with laser excitation and light collection. The objective here is to establish the form of Eq. (6) and to demonstrate that $\beta$ is a relatively small term in the decay profiles and hence, overall, to characterise the absolute rate data of the chemical reactions.

Examples of typical LIF profiles at $\lambda = 420.2$ nm using the ($6^2P_{3/2}$–$5^2S_{1/2}$) Rydberg transition (system A) for the decay of Rb($5^2S_{1/2}$) in the presence of a fluoride, $CH_3F$, and excess He at $T = 780$ K in a mixture of fixed fractional composition, $f = [CH_3F]/([He] + [CH_3F]) = 5.3 \times 10^{-4}$, at varying values of $p_T$ are shown in Fig. 2. Similar sets of LIF profiles taken at this wavelength were recorded for other reactants listed in Section 2. Fig. 3 shows LIF decay profiles for Rb($5^2S_{1/2}$) at $\lambda = 780.0$ nm {Rb($5^2P_{3/2}$) → Rb($5^2S_{1/2}$)} (system B) in the presence of an iodide, $CH_3I$ ($f = 2.2 \times 10^{-4}$), at $T = 875$ K. Solid lines represent the computer fit to the standard form

$$I_F = A + B \exp(-k't) \quad (7)$$

where $I_F$ represents the fluorescence intensity which is directly proportional to the Rb concentration at time $t$ in the standard weak light absorption approximation, and $A$ represents the long-time component of the scattered light. Halogen atom exchange should not be significant when flowing the relatively inert $CH_3F$, heavily diluted in He, over RbBr, chosen for its photochemical yield of Rb($5^2S_{1/2}$). Whilst some halogen exchange could take place with, for example, $CH_3I$ + He and RbBr, it may be emphasised that the current use here of flow systems should minimise this effect with the interaction of reactants prior to photolysis

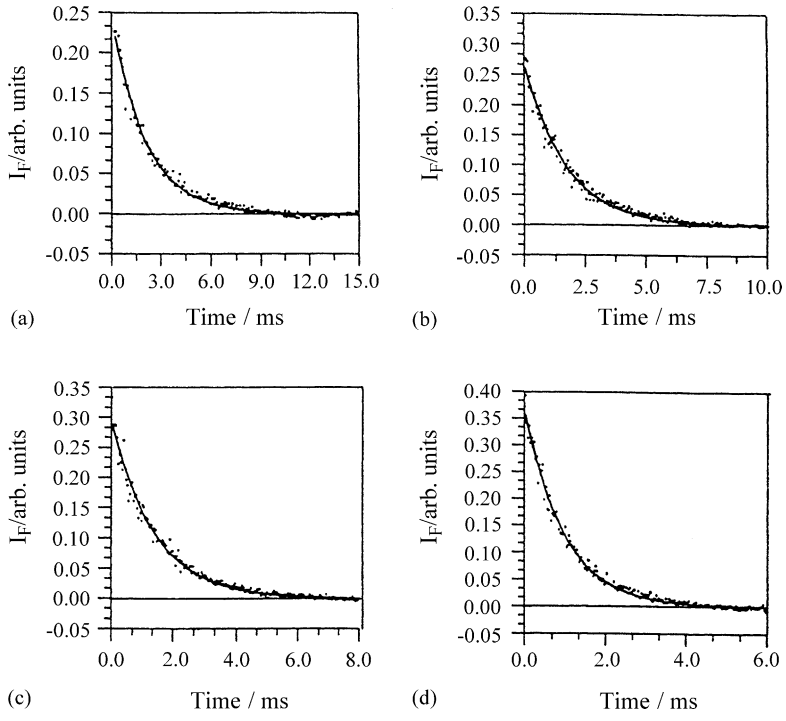


Fig. 2. Examples of the digitised time variation of the LIF intensity at $\lambda = 420.2$ nm {Rb[6p($^2P_{3/2}$)] → Rb[5s($^2S_{1/2}$)]} indicating decay profiles of Rb($5^2S_{1/2}$) atoms, generated by the FP of RbBr vapour at elevated temperature (780 K) in the presence of $CH_3F$ and excess helium buffer gas ($f = [CH_3F]/([CH_3F] + [He]) = 5.3 \times 10^{-4}$) at different total pressures, $p_T$. $p_T$ (Torr): (a) 17.4; (b) 44.1; (c) 71.0; (d) 99.7.

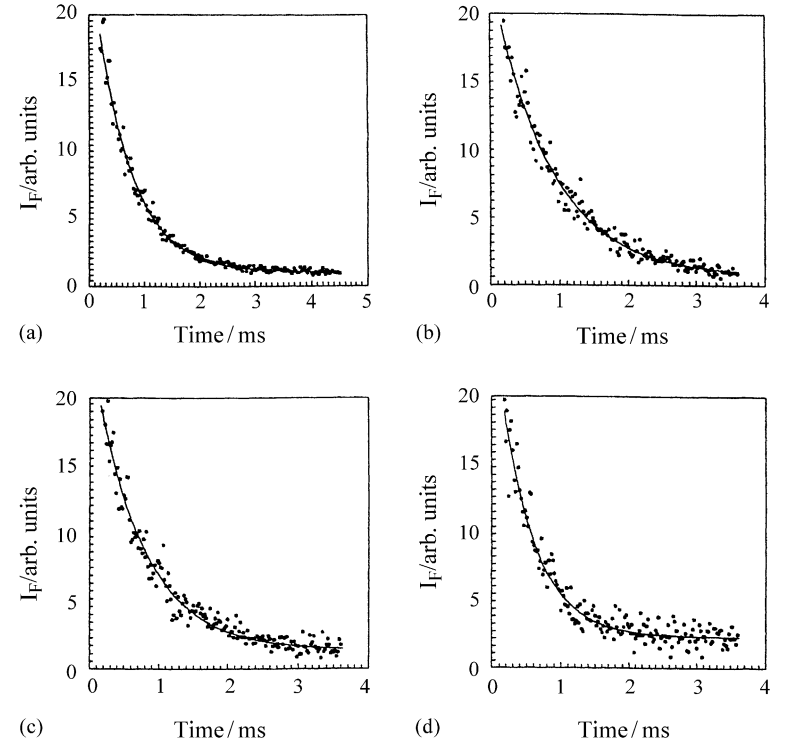


Fig. 3. Examples of the digitised time variation of the LIF intensity at $\lambda = 780.0$ nm {Rb[5s5p($^2P_{3/2}$)] → Rb[5s($^2S_{1/2}$)]} indicating decay profiles of Rb($5^2S_{1/2}$) atoms, generated by the FP of RbI vapour at elevated temperature (875 K) in the presence of $CH_3I$ and excess helium buffer gas ($f = 2.2 \times 10^{-4}$) at different total pressures, $p_T$. $p_T$ (Torr): (a) 14.1; (b) 30.0; (c) 50.1; (d) 70.4.

taking place in the gas phase rather than at a solid surface, as in static systems. Nevertheless, this needs to be borne in mind when considering appropriate rate data. Values of $k'$ from the decay profiles were measured over a wide range of the total pressure for the different reactants in excess He.

### 3.1. Fluorine atom-abstraction

The reactions of $Rb(5^2S_{1/2})$ with $CF_4$, $CF_3H$, $CF_2H_2$ and $CH_3F$ were studied at 780 K using RbBr as the photochemical precursor of $Rb(5^2S_{1/2})$.

$$Rb(5^2S_{1/2}) + CF_xH_{4-x} \rightarrow RbF + CF_{x-1}H_{4-x} \quad (1 \leq x \leq 4) \quad (k_{RX}) \tag{8}$$

The range of the fluorocarbon fractional composition, $f$, used varied from $4.2 \times 10^{-4}$ to 0.1, depending on the compound reactivity. LIF profiles at $\lambda = 420.2$ nm of $Rb(5^2S_{1/2})$ with these reactants were found to be strictly exponential in form and were fitted by a non-linear least-squares fitting routine to Eq. (7). Fig. 4 shows plots of $k'p_T$ vs. ${p_T}^2$ for each fluorocarbon studied here. Values of $k_{RX}$ for the reactions of $Rb(5^2S_{1/2})$ with these fluorides were thus obtained from the slopes of these plots and the appropriate values of $f$. A summary of these results is presented in Table 1 together with analogous rate data derived by other methods and for other alkali atoms. To the best of our knowledge, with the exception of $CF_4$, these absolute rate constants constitute the first values reported for these reactions. The only published kinetic study of the reaction of $Rb(5^2S_{1/2})$ with $CF_4$ is that of Husain and Ji [18] using the FP/ARA method.

### 3.2. Bromine atom-abstraction

Time-resolved FP/LIF measurements, principally using system A ($\lambda = 420.2$ nm) were carried out for kinetic studies

Table 1
Absolute second-order rate constants for the reaction of ground-state rubidium atoms, $Rb(5^2S_{1/2})$, and other alkali metal atoms with a series of halogenated compounds at elevated temperatures determined by time-resolved spectroscopic methods (errors $\pm 2\sigma$)

| Reactant | Alkali metal | $T$ (K) | $k_{RX}$ (cm$^3$ molecule l$^{-1}$ s$^{-1}$) | Detection method |
|---|---|---|---|---|
| $CF_4$ | Na | 833 | $\approx 5.1 \times 10^{-15}$ | ARA[a] |
| | K | 755 | $\approx 8.0 \times 10^{-14}$ | ARA[b] |
| | Rb | 780 | $(4.8 \pm 1.4) \times 10^{-15}$ | LIF[c] |
| | | 744 | $(1.0 \pm 0.2) \times 10^{-14}$ | ARA[d] |
| | Cs | 830 | $(1.9 \pm 0.8) \times 10^{-15}$ | LIF[e] |
| | | 833 | $(7.0 \pm 2.4) \times 10^{-15}$ | ARA[f] |
| $CF_3H$ | Rb | 780 | $(9.9 \pm 1.4) \times 10^{-14}$ | LIF[c] |
| | Cs | 830 | $(3.7 \pm 2.4) \times 10^{-14}$ | LIF[e] |
| | | 833 | $(2.4 \pm 0.4) \times 10^{-12}$ | ARA[f] |
| $CF_2H_2$ | Rb | 780 | $(9.7 \pm 3.4) \times 10^{-13}$ | LIF[c] |
| $CH_3F$ | Na | 780 | $\approx 2.3 \times 10^{-15}$ | ARA[g] |
| | K | 780 | $\approx 2.2 \times 10^{-14}$ | ARA[h] |
| | Rb | 780 | $(1.1 \pm 0.6) \times 10^{-12}$ | LIF[c] |
| | Cs | 834 | $(3.4 \pm 0.8) \times 10^{-12}$ | ARA[f] |
| $CF_3Br$ | Na | 830 | $\approx 8 \times 10^{-11}$ | ARA[a] |
| | K | 830 | $(6.6 \pm 2.6) \times 10^{-11}$ | ARA[b] |
| | Rb | 830 | $(6.8 \pm 0.9) \times 10^{-12}$ | LIF[c] |
| | | 875 | $(1.9 \pm 0.1) \times 10^{-11}$ | LIF[c] |
| | | 874 | $(1.1 \pm 1.2) \times 10^{-11}$ | ARA[d] |
| | Cs | 780 | $(3.8 \pm 2.4) \times 10^{-11}$ | LIF[e] |
| | | 830 | $(2.9 \pm 0.6) \times 10^{-11}$ | ARA[f] |
| $CF_2Br_2$ | Rb | 780 | $(2.9 \pm 1.6) \times 10^{-11}$ | LIF[c] |
| | Cs | 780 | $(1.2 \pm 0.2) \times 10^{-10}$ | LIF[e] |
| $CFBr_3$ | Rb | 780 | $(4.3 \pm 2.8) \times 10^{-11}$ | LIF[c] |
| | Cs | 780 | $(6.4 \pm 0.3) \times 10^{-11}$ | LIF[e] |
| $CH_2Br_2$ | Rb | 876 | $(9.9 \pm 0.1) \times 10^{-12}$ | LIF[c] |
| $C_2H_4Br_2$ | Rb | 876 | $(8.5 \pm 0.2) \times 10^{-12}$ | LIF[c] |
| $CH_3I$ | Rb | 875 | $(1.1 \pm 0.1) \times 10^{-11}$ | LIF[c] |
| $CH_2I_2$ | Rb | 876 | $(9.1 \pm 0.1) \times 10^{-12}$ | LIF[c] |

[a] Ref. [10].
[b] Refs. [26,27].
[c] This work.
[d] Ref. [18].
[e] Refs. [20,28].
[f] Ref. [29].
[g] Ref. [10].
[h] Ref. [27].

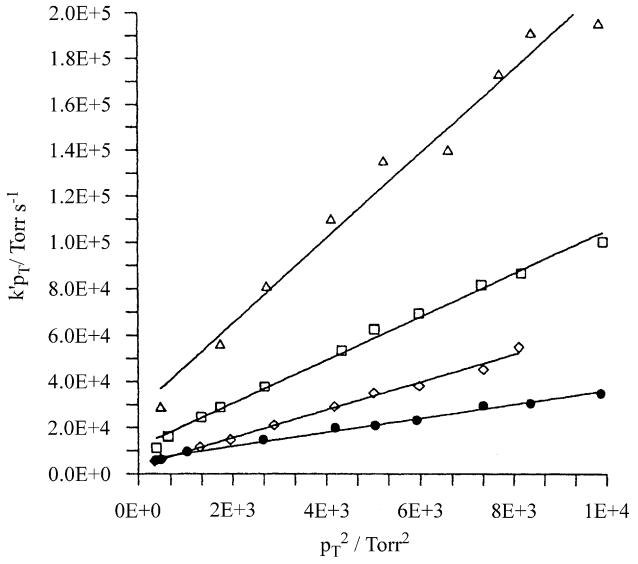


Fig. 4. Variation in the first-order decay coefficient $k'$ for the decay of $Rb(5^2S_{1/2})$ obtained from time-resolved LIF monitoring at $\lambda = 420.2$ nm $\{Rb[6p(^2P_{3/2})] \rightarrow Rb[5s(^2S_{1/2})]\}$ following the FP of RbBr vapour at $T = 780$ K in the presence of $CF_4$, $CF_3H$, $CF_2H_2$ and $CH_3F$ with excess helium buffer gas at different total pressure, $p_T$ ($k'p_T$ vs. $p_T^2$; solid lines are linear least-squares fits to the data). (●) $CF_4$, $f = 3.7 \times 10^{-2}$; (△) $CF_3H$, $f = 2.5 \times 10^{-2}$; (□) $CF_2H_2$, $f = 8.1 \times 10^{-4}$; (◇) $CH_3F$, $f = 8.3 \times 10^{-4}$.

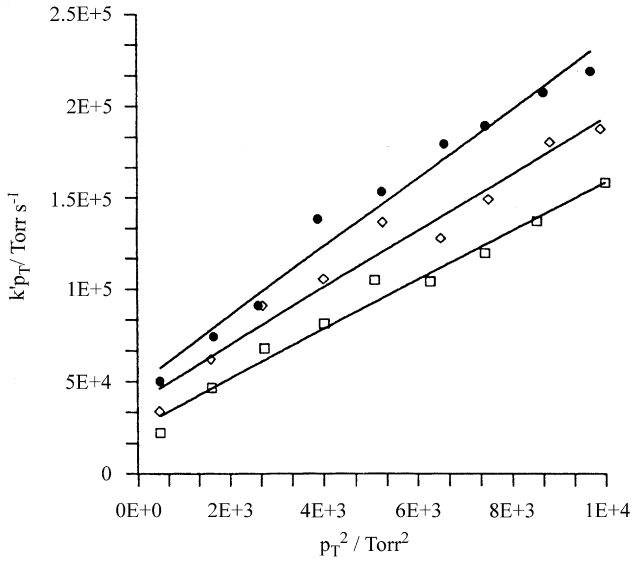


Fig. 5. Variation in the first-order decay coefficient $k'$ for the decay of $Rb(5^2S_{1/2})$ obtained from time-resolved LIF monitoring at $\lambda = 420.2$ nm $\{Rb[6p(^2P_{3/2})] \rightarrow Rb[5s(^2S_{1/2})]\}$ following the FP of RbBr vapour at $T = 780$ K in the presence of $CF_3Br$, $CF_2Br_2$ and $CFBr_3$ with excess helium buffer gas at different total pressure, $p_T$ ($k'p_T$ vs. $p_T^2$; solid lines are linear least-squares fits to the data). (●) $CF_3Br$, $f = 1.7 \times 10^{-4}$ ($T = 830$ K); (□) $CF_2Br_2$, $f = 5.6 \times 10^{-5}$ ($T = 780$ K); (◇) $CFBr_3$, $f = 4.8 \times 10^{-5}$ ($T = 780$ K).

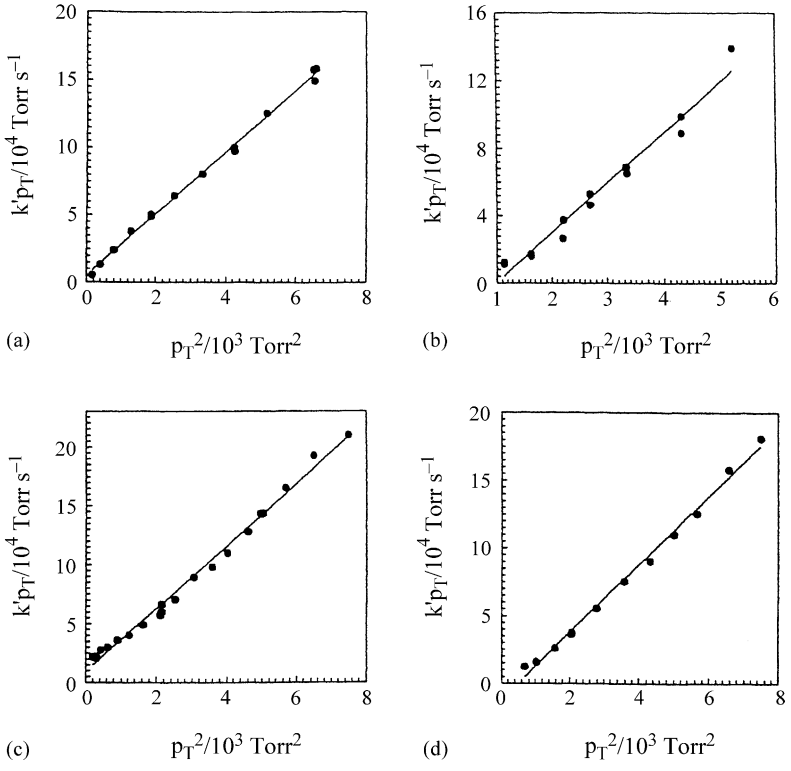


Fig. 6. Variation in the first-order decay coefficient $k'$ for the decay of $Rb(5^2S_{1/2})$ obtained from time-resolved LIF monitoring at $\lambda = 780.0$ nm $\{Rb[5s5p(^2P_{3/2})] \rightarrow Rb[5s(^2S_{1/2})]\}$ following the FP of RbI vapour in the presence of $CH_2Br_2$, $C_2H_4Br_2$, $CH_3I$ and $CH_2I_2$ with excess helium buffer gas at different total pressure, $p_T$ ($k'p_T$ vs. $p_T^2$; solid lines are linear least-squares fits to the data). (a) $CH_2Br_2$, $f = 2.1 \times 10^{-4}$ ($T = 876$ K); (b) $C_2H_4Br_2$, $f = 3.2 \times 10^{-4}$ ($T = 876$ K); (c) $CH_3I$, $f = 2.2 \times 10^{-4}$ ($T = 875$ K); (d) $CH_2I_2$, $f = 2.5 \times 10^{-4}$ ($T = 876$ K).

of the reactions

$$Rb(5^2S_{1/2}) + CF_yBr_{4-y} \rightarrow RbBr + CF_yBr_{3-y} \quad (1 \leq y \leq 3) \quad (k_{RX}) \quad (9)$$

and were performed under pseudo-first-order conditions working with $f$ factors typically between $2.5 \times 10^{-5}$ and $4.0 \times 10^{-4}$ according to the halogen reactivity. The reaction of $Rb(5^2S_{1/2})$ with $CF_3Br$ was studied at both 830 K (system A, $\lambda = 420.2$ nm) and 875 K (system B, $\lambda = 780.0$ nm). As in the study of fluorine atom-abstraction reactions, RbBr was used as the photochemical precursor of the Rb atoms. LIF profiles were recorded at $\lambda = 780.0$ nm (B) for the decay of $Rb(5^2S_{1/2})$ in the presence of other reactant gases listed in Section 2 . Fig. 5 shows linear plots of $k'p_T$ vs. ${p_T}^2$ following Eq. (6) for the reactions of $Rb(5^2S_{1/2})$ with $CF_3Br$, $CF_2Br_2$ and $CFBr_3$ from LIF measurements taken at $\lambda = 420.2$ nm. Fig. 6a and b shows analogous plots from data taken at $\lambda = 780.0$ nm for the reactions of $Rb(5^2S_{1/2})$ with $CH_2Br_2$ and $C_2H_4Br_2$. The slopes of these plots coupled with the appropriate values of $f$ yield the absolute second-order rate constants for these reactions of atomic rubidium at the temperatures listed in Table 1. Only $k_{CF_3Br}$ has been previously determined using the FP/ARA technique [18]. To the best of our knowledge, absolute rate data have not been reported for the reactions of $Rb(5^2S_{1/2})$ with the remaining bromides.

### 3.3. Iodine atom-abstraction

A set of LIF measurements at $\lambda = 780.0$ nm, analogous to those shown for $Rb(5^2S_{1/2}) + CH_3I$ in Fig. 3, were recorded for the decay atomic rubidium in the presence of $CH_2I_2$ at $T = 876$ K ($f = 2.5 \times 10^{-4}$). Fig. 6 includes the plots of $k'p_T$ vs. ${p_T}^2$ for the reaction of $Rb(5^2S_{1/2})$ with $CH_3I$ and $CH_2I_2$ yielding the absolute second-order rate constants for these reactions using the values of $f$ employed. The results obtained for the reactions investigated here (errors $\pm 2\sigma$) are listed in Table 1 together with the previous analogous data, where available, reported for reactions of $Na(3^2S_{1/2})$, $K(4^2S_{1/2})$ and $Cs(6^2S_{1/2})$.

## 4. Discussion

Table 1 lists the absolute second-order rate constants for the fluorine, bromine and iodine atom-abstraction reactions by $Rb(5^2S_{1/2})$ studied in this investigation together with data for analogous reactions of other alkali metal atoms using the FP/ARA or FP/LIF time-resolved techniques. Fluorine atom-abstraction reactions are slower than those for bromine and iodine atoms with the reactivity increasing as the number of fluorine atoms in the reactant molecules decreases. The only previous results reported for the reactions of atomic rubidium investigated here are for $CF_4$ and $CF_3Br$, both employing the FP/ARA method, are larger than the LIF data described here. The LIF data are favoured in view of the use of flow systems, as indicated in Section 2, and the accompanying data acquisition and signal averaging procedure. The comparison of the absolute rate constant for the Br atom-abstraction with $CF_3Br$, $k_{CF_3Br}$, for $Rb(5^2S_{1/2})$ with the analogous result for $Cs(6^2S_{1/2})$, also determined by LIF in our laboratory [20,21], shows that the latter is clearly greater and consistent with the smaller ionisation potential of the caesium atom compared to atomic rubidium [30], although this kind of relationship is not consistently observed across all the measurements. For analogous comparisons in Table 1, FP/LIF data are, in general, preferred to those derived from the FP/ARA technique in view of the advantages of the flow method and the avoidance of complexities arising from the use of a static reactor in the ARA method operating in the 'single-shot mode'.

As has been previously noted, measurements of the presented type using both A and B systems are usually single-temperature measurements in the range 780–875 K, where a clear dependence of $k_{RX}$ on temperature is difficult to characterise when endeavouring to extract a small activation energy from measurements at elevated temperatures. Hence, activation energies were estimated assuming an approximate Arrhenius pre-exponential factor equal to the collision number ($\approx 2 \times 10^{-10}$ cm$^3$ molecule$^{-1}$ s$^{-1}$) which is often employed for reactions of atoms and small radicals [21]. In the case of the $Rb + CF_3Br$ results, this procedure yields $E_a = 23$ and 17 kJ mol$^{-1}$ for $T = 830$ and 875 K, respectively. The use of the Arrhenius equation with these data (Table 1) yields $E_a = 22$ kJ mol$^{-1}$, though this level of agreement is considered to be fortuitous with this method involving two separate FP/LIF apparatus employing different atomic resonance transitions for LIF monitoring across a narrow range at elevated temperature.

Reaction enthalpies were calculated using the R–X bond dissociation energies and the corresponding bond energy of Rb halide formed in the reaction ($D$(R–X) (kJ mol$^{-1}$): $CF_3$–F, 541.2; $CF_2H$–F, 527.1; $CFH_2$–F, 492.9; $CH_3$–F, 452 ± 13; $CF_3$–Br, 295.4 ± 13 and $CH_3$–I, 222.6 [30–33]. With the exceptions of $CF_4$ and $CF_3H$, the halogen atom-abstraction reactions are exothermic in all cases. Hydrogen atom-abstraction reactions of $Rb(5^2S_{1/2})$ with hydrofluoromethanes are highly endothermic ($\Delta H$ (kJ mol$^{-1}$) $CF_3H$, 279.4 ± 17; $CH_2F_2$, 264 ± 17; $CH_3F$, 256.8 ± 17) [30,31] and may be neglected. Bond dissociation energies for $CF_2Br_2$ and $CFBr_3$ were not found in literature but the exothermicity for reaction with $Rb(5^2S_{1/2})$ should be greater than $-85 \pm 9$ kJ mol$^{-1}$, the value of $\Delta H$ value calculated for $CF_3Br$ [30]. Br atom-abstraction reactions of $Rb(5^2S_{1/2})$ with fluorobromomethanes are favoured over those involving F atom-abstraction on thermochemical grounds. Whilst we may note trends such as for F atom-abstraction with the series, $k_{CF_4} < k_{CF_3H} < k_{CF_2H_2} < k_{CH_3F}$ and Br atom-abstraction for the limited series, $k_{CF_3Br} < k_{CF_2Br_2} < k_{CFBr_3}$, simple correlations are difficult to assign across a limited range of rates for the remaining

Br and I-containing reactants. An analogous variation of the rate data for Cs($6^2S_{1/2}$) with an increase in reactivity observed for the reactions of fluorine-containing molecules with the decrease in the number of F atoms in the reactant molecule has also been observed [20,21] and is consistent with the thermochemistry of the reactions. Overall, the present measurements have led to a new body of absolute rate data for reaction of atomic rubidium from direct monitoring in the time-domain using FP combined with LIF.

## Acknowledgements

We thank the Spanish Direccion General de Investigacion Cientifica y Tecnica (Project PB94-0744) for financial support. K.M.N. De Silva thanks the Association of Commonwealth Universities, the Commonwealth Commission (London) and the British Council for an Academic Staff Commonwealth Scholarship during the tenure of which this work was carried out.

## References

[1] J.M.C. Plane, in: A. Fontjin (Ed.), Gas-phase Metal Reactions, Elsevier, Amsterdam, 1992.
[2] J.M.C. Plane, Int. Rev. Phys. Chem. 10 (1991) 55.
[3] D. Husain, J. Chem. Soc., Faraday Trans. II 85 (1989) 85.
[4] S.A. Edelstein, P. Davidovits, J. Chem. Phys. 55 (1971) 5564.
[5] J. Maya, P. Davidovits, J. Chem. Phys. 59 (1973) 3143.
[6] J. Maya, P. Davidovits, J. Chem. Phys. 61 (1974) 1082.
[7] P. Davidovits, in: P. Davidovits, D.L. McFadden (Eds.), Alkali Halide Vapours, Academic Press, New York, 1979, p. 331.
[8] D. Husain, J.M.C. Plane, J. Chem. Soc., Faraday Trans. II 78 (1982) 163.
[9] D. Husain, J.M.C. Plane, J. Chem. Soc., Faraday Trans. II 78 (1982) 1175.
[10] D. Husain, P. Marshall, J.M.C. Plane, J. Chem. Soc., Faraday Trans. II 81 (1985) 301, D. Husain, P. Marshall, Int. J. Chem. Kinet. 18 (1986) 83.
[11] D. Husain, Y.H. Lee, P. Marshall, Combust. Flame 68 (1987) 143.
[12] D. Husain, J.M.C. Plane, C.C. Xiang, J. Chem. Soc., Faraday Trans. II 81 (1985) 561.
[13] J.M.C. Plane, D. Husain, J. Chem. Soc., Faraday Trans. II 82 (1986) 897.
[14] S.A. Carl, K.M.N. De Silva, D. Husain, Z. Phys. Chem. 203 (1998) 113.
[15] K.M.N. De Silva, D. Husain, Photochem. Photobiol. A 111 (1997) 1.
[16] E. Martínez, J. Albaladejo, A. Notario, E. Jiménez, D. Husain, J. Mol. Struct. 410 (1997) 73.
[17] D. Husain, B. Ji, Combust. Flame 79 (1990) 250.
[18] D. Husain, B. Ji, J. Photochem. Photobiol. A 48 (1989) 1.
[19] E. Martínez, J. Albaladejo, A. Notario, D. Husain, J. Photochem. Photobiol. A 95 (1996) 103.
[20] A. Notario, Ph.D. Thesis, Universidad de Castilla-La Mancha, 1996.
[21] E. Martínez, J. Albaladejo, A. Notario, D. Husain, J. Chem. Res. (1996) S, 16; M, 364.
[22] J.E. Mayer, I.H. Winter, J. Chem. Phys. 6 (1938) 301.
[23] R.C. Miller, P. Kusch, J. Chem. Phys. 25 (1956) 860.
[24] C.E. Cogin, G.E. Kimball, J. Chem. Phys. 16 (1948) 1035.
[25] P. Davidovits, D.C. Brodhead, J. Chem. Phys. 46 (1967) 2968.
[26] D. Husain, Y.H. Lee, J. Chem. Soc., Faraday Trans. II 83 (1987) 2325.
[27] D. Husain, Y.H. Lee, Int. J. Chem. Kinet. 20 (1998) 223.
[28] E. Martínez, J. Albaladejo, A. Notario, E. Jiménez, D. Husain, Combust. Flame 107 (1996) 299.
[29] R.S. Clay, D. Husain, J. Chem. Res. (1990), S 384, M 2994.
[30] D.R. Lide, in: CRC Handbook of Chemistry and Physics, 78th Edition, CRC Press, Boca Raton, FL, 1997.
[31] W.B. Demore, S.P. Sander, C.J. Howard, A.R. Ravishankara, D.M. Golden, C.E. Kolb, R.F. Hampson, M.J. Kurylo, M.J. Molina, in: Chemical Kinetics and Photochemical Data for Use in Stratospheric Modelling, JPL Publication 97-4, Jet Propulsion Laboratory, Pasadena, CA, 1997.
[32] V.I. Vedeneyev, L.V. Gurvich, V.N. Kondratiev, V.A. Medvedev, Ye.L. Frankevitch, Bond Energies, Ionisation Potential and Electron Affinities, Nauka, Moscow, 1974.
[33] J.R. Majer, C.R. Patrick, J.C. Robb, Trans. Faraday Soc. 57 (1961) 14.